IEEE Access
Multidisciplinary | Rapid Review | Open Access Journal

Received August 9, 2019, accepted August 18, 2019, date of publication August 26, 2019, date of current version September 18, 2019.

Digital Object Identifier 10.1109/ACCESS.2019.2937668

Longitudinal and Lateral Trajectory Planning for the Typical Duty Cycle of Autonomous Load Haul Dump

QING GU, LI LIU, GUOXING BAI, KAILUN LI, YU MENG, AND FEI MA
School of Mechanical Engineering, University of Science and Technology Beijing, Beijing 100083, China

Corresponding author: Qing Gu (qinggu@ustb.edu.cn)

This work was supported in part by the National Key Research and Development Program of China under Grant 2018YFC0604403 and Grant 2016YFC0802905, and in part by the Fundamental Research Funds for the Central Universities under Grant FRF-TP-17-010A2.

ABSTRACT With the development of intelligent mining, autonomous driving will be the basic function of intelligent Load Haul Dump (LHD). Trajectory planning is the key part of autonomous driving. Due to the articulated structure, the motion state variables of the front and rear bodies are strongly nonlinear, leading to complex nonlinear collision avoidance constraints. In addition, the articulated angle and angular velocity of the LHD have physically constraints. At the same time, the terminal attitude constraint should be considered since LHD is a mining equipment. All these factors bring great difficulties to LHD trajectory planning and none of the existing methods can deal with these factors directly. In order to solve these problems, according to the most common working scenario, a novel trajectory planning method is proposed for autonomous LHD based on numerical optimization, leading to a safe and feasible time-space trajectory for efficient production. The novelty of this work is the introduction of a longitudinal and lateral trajectory planning for the typical duty cycle of LHD. More importantly, by the ingenious concept for modeling, there are two salient features of the proposed method. Firstly, no angles are used as the decision variable, and secondly, the collision constraints of the rear car are not directly considered. Through this way, the number of nonlinear constraints and the complexity of the model can keep in a reasonable level, which makes the model easy to solve. At the same time, by giving the collision-free condition and limiting the heading angular velocity, the generated trajectory is collision-free and satisfies the physical constraints of articulated angle. Case studies confirm the effectiveness of the proposed method. Adopting the proposed method to generate a spatiotemporal trajectory is beneficial to ensure safety and improve production efficiency.

INDEX TERMS Articulated vehicle, kinematics constrains, load-haul-dump (LHD), nonlinear constrains, trajectory plan.

I. INTRODUCTION

In order to guarantee the worker safety, increase the mining efficiency and reduce production cost, intelligent mining became the development direction of mining industry. As the main equipment for underground metal mining operation, automation of Load Haul Dump (LHD) plays a very important role in intelligent mining. LHD is a kind of low body vehicle specially designed for underground work. It is a central articulated, loading, transportation, dumping joint operation equipment that suits for the limited underground working space. Fig.1 shows an LHD in underground tunnel. Autonomous driving is the basic and necessary function of intelligent automatic LHD.

Usually, there are mainly two ways to achieve automatic driving. One is to apply reactive navigation. In this case, the route in the underground tunnel can be depicted by a sequence of nodes and road segments. Wall following method combined with driving tips [1] can achieve autonomous driving. The other is to apply absolute navigation. In this case, a path or a trajectory should be planned at first, and then LHD needs to track the path through some control methods to achieve autonomous driving. In this circumstance, the path is usually represented by a series of path coordinate points.

The associate editor coordinating the review of this article and approving it for publication was Tai-hoon Kim.

FIGURE 1. Load Haul Dump (LHD).

A. MOTIVATIONS

In mining process, in order to ensure safety and production efficiency, LHD should carry out production tasks according to the working plan (Scheduling layer) and the dispatching command. When LHD is driving manually (including remote control), an experienced driver can determine in the right velocity according to the dispatching command and the tunnel shape. For example, the LHD may slow down and increase the turning radius of the trajectory when turning at the intersection, at the same time, LHD will keep a certain distance with the tunnel wall. However, for autonomous LHD, all these work needs to be done automatically, which requires not only location information, but also velocity information, such as a v-t trajectory in time dimension. Moreover, except work solely, LHD often needs to cooperate with other mining equipment. For example, LHD and underground dump truck usually work together. In this case, attitude is also an important factor need to be considered. Base on the analysis above, generating a target trajectory with the information of position, attitude and velocity is an urgent problem to be solved for autonomous LHD.

B. RELATED WORKS

At present, motion plan about LHD mainly focus on path plan. A great amount of path plan algorithms can be used to find the optimal path between the start point and end point. These planning techniques can be classified in three groups: graph search, interpolating and numerical optimization [2], [3]. For example, we can obtain the shortest path between two points by Dijkstra or A*algorithm on a discrete cell-grid, lattices or topological map [2]. Moreover, a smooth or high order continuous path can be obtained by using interpolating curve algorithms, such as Lines and Circles, Clothoid Curves or Bézier Curves [2]. According to the characteristics of the LHD, Anderson *et al.* [4] obtained a LHD's path through symmetric X4Y4 curve, the curvature and its derivatives are continuous, which improved the tracking speed and accuracy. Ma *et al.* [5] proposed an improved A*algorithm for intelligent LHD path planning. The nodes are expended according to the articulated angle, which leads to a more acceptable path. At the same time, a heuristic collision risk cost is designed to avoid collision between LHD and the tunnel walls. Choi and Huhtala [6] planned a collision free smooth path by comprehensively utilized State Lattice, Bezier curves and A*algorithm. In an open environment without considering collision, Ishimoto *et al.* [7], Yossawee *et al.* [8] proposed a path plan algorithm, by which the curvature continuous paths among the loading, dumping and reversing point could be obtained based on symmetric clothoid curves. The generated path is easy to be followed. Nayl *et al.* [9], [10] proposed a on line path planning method based on a MP controller under a constant velocity in an arena with fixed obstacles, and sensitivity analysis shows the effect of kinematic parameters on the method.

Based on the existing literatures, it is known that many good results have been obtained. However, planning methods specifically for the characteristics of LHD are still insufficient.

LHD is mainly working in the narrow underground metal mine. The main work for LHD is to move the ores from the loading point to the dumping point (during this process, a reversing point is needed). Therefore, it is driving back and forth in a local area. The major work scenarios of LHD can be seen as an "L" duty cycle and the schematic is shown in Fig. 2.

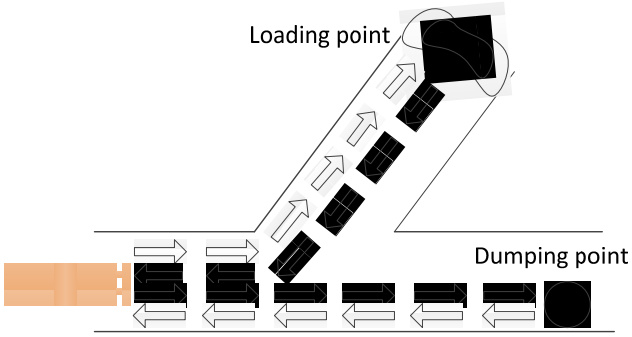

FIGURE 2. "L" duty cycle of LHD.

In Fig. 2, the black arrows represent heavy haulage and the white arrows represent no loading from the dumping point back to the loading point. The dumping point is an ore pass or an underground dump truck which is located in the haulage way. The loading point is a pile of ore and it is moving forward with the tunnel's digging. LHD executes "L" duty cycle repetitively between the loading point and the dumping point in underground tunnel for a long period, usually several weeks even several months. During this process, the loading point is moving and the dumping point is fixed.

It can be seen that LHD will repeatedly pass the junction during working. When LHD is steering, it is not enough to only provide the path (position information), velocity is the other important factor. If the velocity is too high, LHD may collide with the tunnel wall. At present, the common way is to set a low velocity value. LHD will keep this velocity for the whole journey or decelerate below this value before turning, and then may reaccelerate after tuning. However, the

speed value is set based on experience, which may reduce the production efficiency and increase energy consumption.

Trajectory plan for intelligent vehicle has been studied extensively and deeply [2], [11]. A lot of trajectory planning methods have been proposed, such as: potential field algorithms [12]–[14], Randomized sampling based methods (Probabilistic Road Maps, RRT and RRT*) [15]–[17], search based methods (A * family [18], [19], state lattices [20]–[22]), optimal control and graph search based method [23], numerical optimization based methods [24]–[28].

Each method has its own characteristics and applicable problem. Without considering the kinematics, by potential field algorithms, we can obtain the collision free trajectory. State lattices can handle several dimensions problem, however, this planer is resolution completed. Therefore, the attitude requirement of the terminal cannot be considered. Based on the same reason, randomized sampling based methods and search based methods cannot handle the problem with the terminal attitude requirements.

In order to guarantee the feasibility of the trajectory, kinematics should be taken into consideration during trajectory planning. At the same time, for LHD trajectory planning, the terminal attitude constraints should be included. In this case, numerical optimization based method is a good choose due to its ability for handling system constraints and nonlinearities. In this method, the trajectory planning problem will be transformed into nonlinear programming problems fully or partially.

For the nonlinear programming problem, Sequential Quadratic Programming (SQP) is a good way to find the solution [25], [29]. Recently, Convex Feasible Set (CFS) algorithm was proposed to solve optimization based trajectory planning problems with convex objective functions and nonconvex constraints [27], [28]. The main idea of the CFS algorithm is to transform the original problem into a sequence of convex subproblems. The idea is similar to SQP in that it tries to solve several convex subproblems iteratively. The difference between CFS and SQP lies in the way to obtain the convex subproblems. SQP obtain the subproblems by Taylor expansion. CFS obtain the subproblems by obtaining CFSs within the nonconvex domain, which is fully considered the geometric structure of the original problem. Since CFS is specifically designed for trajectory planning problem, it is more efficient for solving [27].

Except the solving algorithms, modeling the trajectory planning problem into convex optimization models directly is the other way. For example, according to a general passenger vehicle in the structured road environment, the trajectory planning problem is decoupled into longitudinal and lateral trajectory planning problems [30]. In each dimension, the trajectory planning problem are modeled as a quadratic programming problem, which is easy to be solved.

However, for LHD working in a narrow tunnel, the collision avoidance constraints of the two bodies must be considered simultaneously. The relationship between the state variables of the front and rear body are nonlinear due to the articulated structure. Therefore, there will be a plenty number of nonlinear constraints (two times more than the number of collision avoidance constraints for a rigid body vehicle) and leads to a nontrivial computational burden to solve the optimization problem.

C. CONTRIBUTIONS

In order to overcome the aforementioned problem and generate an optimal trajectory for LHD in ''L'' duty cycle, a trajectory planning method based on longitudinal and lateral trajectory planning is proposed. Through rational design, only the state variables of the front body are chosen as decision variables. Furthermore, a Theorem for the rationality condition of LHD trajectory is proposed and proved, through which collision avoidance constraints of the rear body are not presented in the trajectory planning model directly, therefore, the number of the constraints can keep in a reasonable level. At the same time, no angles are included as the decision variable, which reduce the complexity of the constraints.

In the proposed method, the complex nonlinear characteristic of articulated vehicle are utilized effectively and the physical limitation of the articulated angle and the angular velocity, as well as the collision avoidance conditions of the rear body can be considered appropriately. Therefore, a reasonable and feasible spatiotemporal trajectory can be obtained conveniently.

The remainder of this paper is structured as follows. Chapter II describe the problem problems to be solved and the kinematics of LHD, and chapter III shows the problem analysis and the basic concept of algorithm design. Chapter IV shows the details of the proposed method. Chapter V gives the case studies to validate the effectiveness of the proposed method, and chapter VI concludes the paper.

II. PROBLEM DESCRIPTION AND KINEMATICS OF LHD

A. PROBLEM DESCRIPTION

LHD has a front body and a rear body. Steering is achieved by controlling the articulated angle. In underground metal mine, the main duty of LHD is to move ore between different working points, which can be called as ''L'' duty cycle, the schematic is shown in Fig.2. Therefore, passing through the junction is one of the most common scenario.

This article investigates time constraint safety trajectory planning problem for this most common scenario of LHD. we want to obtain a reasonable trajectory including position and velocity. When LHD is tuning in the junction, it is easy to collide with the tunnel wall without considering the velocity. In order to avoid this situation, kinematics should be considered in trajectory planning. During planning, the following constraints should be satisfied.

- Both of the two bodies of LHD need to keep a certain distance from tunnel wall in the underground tunnel;
- The speed limit of LHD in underground tunnel;

- The constraints of LHD physical and design characteristics;
- The position and attitude constraints of the vehicle in the end point.

B. KINEMATICS of LHD

LHD has an articulated structure. Therefore, the description of its attitude is different from that of rigid vehicles, both of the heading angle and the articulated angle need to be considered during motion plan.

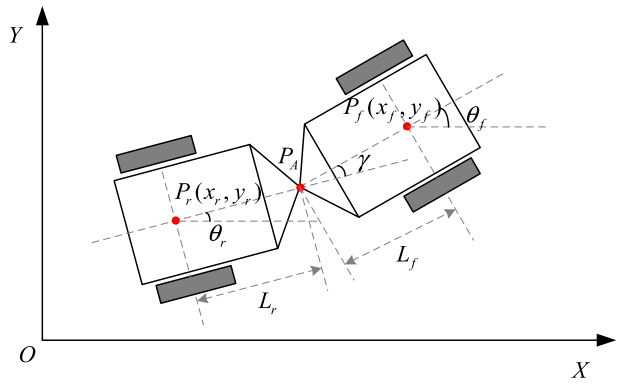

FIGURE 3. The structure of LHD.

The structure of LHD is shown in Fig. 3. There are two bodies. P_A is the articulated point. $P_f(x_f, y_f)$ is the axle center of the front body. $P_r(x_r, y_r)$ is the axle center of the rear body. The heading angles of the front body and rear body are θ_f and θ_r, respectively. The distance between P_A and P_f is L_f. The distance between P_A and P_r is L_r.

The articulated angle γ is the difference between θ_f and θ_r

$$\gamma = \theta_f - \theta_r. \tag{1}$$

The position relationship between P_f and P_r is

$$x_r = x_f - L_f \cos\theta_f - L_r \cos\theta_r, \tag{2}$$

$$y_r = y_f - L_f \sin\theta_f - L_r \sin\theta_r, \tag{3}$$

Based on literature [9], with the assumption that no side slip, kinematic model can be depicted as

$$\begin{bmatrix} \dot{x}_f \\ \dot{y}_f \\ \dot{\theta}_f \\ \dot{\gamma} \end{bmatrix} = \begin{bmatrix} \cos\theta_f & 0 \\ \sin\theta_f & 0 \\ \dfrac{\sin\gamma}{L_f\cos\gamma + L_r} & \dfrac{L_r}{L_f\cos\gamma + L_r} \\ 0 & 1 \end{bmatrix} \begin{bmatrix} v_f \\ \dot{\gamma} \end{bmatrix}$$

where $\dot{\gamma}$ is the angular velocity of articulated angle γ. The angular velocity of the front body is

$$\dot{\theta}_f = \frac{v_f \sin\gamma + l_r\dot{\gamma}}{l_f\cos\gamma + l_r}, \tag{4}$$

The physical constraints of the articulated angle and its velocity are

$$\gamma_{\min} \le \gamma \le \gamma_{\max}, \tag{5}$$

$$\dot{\gamma}_{\min} \le \dot{\gamma} \le \dot{\gamma}_{\max}. \tag{6}$$

III. PROBLEM ANALYSIS AND ALGORITHM DESIGN CONCEPT

In order to consider the kinematics and the terminal attitude requirements, numerical optimization method can be applied. However, from equation (2) to (6), it can be seen that the motion equations are highly nonlinear, trigonometric functions are included. There are three important angles, which are the heading angles of the front and rear body, as well as the articulated angel. LHD is an engineering equipment, therefore, the heading angle of the front body and the articulated angel have requirements at the end point. Based on this analysis, usually, both of the two car bodies' state variables, or the angels and one of the car body's state variables should be chosen as the decision variables for the optimization problem. Therefore, trigonometric relation bring nonlinear constraints that make the problem more complex.

Moreover, since there are two car bodies, the number of the constraints (including the kinematic, the terminal condition and the boundaries) of the optimization problem is more than twice of the number of the constraints of a rigid vehicle. Therefore, it is a nontrivial computational burden for solving such an optimization problem.

Therefore, in order to reduce the computational burden, it is better to reduce the number and the complexity of the constraints. Based on the analysis, the complexity is mainly caused by the nonlinear relationship between the front and rear bodies. Therefore, if only one car body's variable appears in the optimization model and the collision free requirement of the other car body can be satisfied simultaneously, the number of the constraints will be reduced. In addition, if on angles are included in the model, the complexity of the constraints will be reduced.

Based on the above analysis, we decompose the original trajectory problem into two dimensions, which are longitudinal and lateral direction. Only the position, velocity and acceleration of the axle center of the front body are chosen as the decision variable, based on which the longitudinal trajectory planning can be modeled as a convex optimization problem. The lateral trajectory planning is based on the result of the longitudinal trajectory. Since no angles are chosen as the decision variables, the constraints about the articulated angel can be satisfied by limiting the angular velocity of the heading angle. Moreover, a theorem is found and proved, through which the safety of the rear body can be guaranteed while the collision avoidance constraints of the rear body are not considered directly in the planning models.

Through the proposed method, nonlinear characteristic of articulated vehicle can be considered appropriately, the nonlinear constraints are extremely reduced, leading to a computationally inexpensive model and a more practical approach

for implementation. Chapter 4 show the details of the novel trajectory method.

IV. TRAJECTORY PLANNING METHOD

In order to plan trajectory, a reference coordinate system should be built. Taking the LHD driving direction in tunnel A as the positive direction of the X-axis, a Cartesian coordinate is established and it is shown in Fig. 4. The horizontal axis of the Cartesian coordinates is parallel to tunnel A. O is the origin of coordinates. The angle between the two tunnels is α. L_{safe} is the safe distance between the tunnel wall and LHD, therefore, the blue area is the feasible area of the LHD. P_f is the axle center of the front body. The blue dotted line is the centerline of the roadway. The coordinates of P_f in the start point and end point are defined as $P_f(X_{fs}, Y_{fs})$ and $P_f(X_{fe}, Y_{fe})$, respectively.

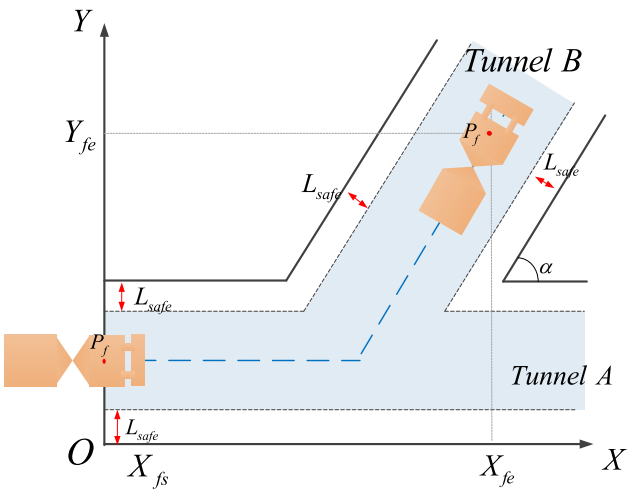

FIGURE 4. Longitudinal bounds of the trajectory.

A. LONGITUDINAL TRAJECTORY PLAN

1) DETERMINE THE LONGITUDINAL BOUNDS

The longitudinal trajectory is planned at first. The longitudinal upper and lower bounds for P_f are determined as

$$x_{\min} = X_{fs}, \quad x_{\max} = X_{fe}. \tag{7}$$

2) OBJECTIVE FOR THE LONGITUDINAL TRAJECTORY

The objective is to minimize the error between the velocity and the desired velocity, as well as the acceleration and the error between two successive accelerations. Therefore, the objective can be written as a quadratic function

$$J = \sum_{i=0}^{N} [\lambda_1 (v_{x_i} - v_{xdes})^2 + \lambda_2 a_{x_i}^2 + \lambda_3 \Delta a_{x_i}^2], \quad i = 0, \ldots\ldots, N, \tag{8}$$

where $\lambda_i, i = 1, 2, 3$ are the weight coefficients, $0 < \lambda_i < 1 \lambda_1 + \lambda_2 + \lambda_3 = 1$; x_i is the longitudinal position of P_f; v_{x_i} is the longitudinal velocity of P_f in x_i; v_{xdes} is the desired longitudinal velocity; a_{x_i} is the longitudinal acceleration of P_f in x_i;$\Delta a_{x_i} = a_{x_i} - a_{x_{i-1}}$.

3) CONSTRAINTS FOR THE LONGITUDINAL TRAJECTORY

In order to describe the constraints, the driving time of LHD are discretized into N time intervals

$$N = T / \Delta t \tag{9}$$

where T is the driving time; Δt is the time interval.

The longitudinal motion can be depicted by

$$x_{i+1} = x_i + v_{x_i} \Delta t + \frac{\Delta t^2}{2} a_{x_i}, \quad i = 0, \ldots\ldots, N, \tag{10}$$

$$v_{x_{i+1}} = v_{x_i} + a_{x_i} \Delta t, \quad i = 0, \ldots\ldots, N, \tag{11}$$

In addition, LHD should satisfy the following constraints

$$x_{\min} \le x_i \le x_{\max}, \quad i = 0, \ldots\ldots, N, \tag{12}$$

$$v_{x\min} \le v_{x_i} \le v_{x\max}, \quad i = 0, \ldots\ldots, N, \tag{13}$$

$$a_{x\min} \le a_{x_i} \le a_{x\max}, \quad i = 0, \ldots\ldots, N, \tag{14}$$

$$\Delta a_{x\min} \le \Delta a_{x_i} \le \Delta a_{x\max}, \quad i = 0, \ldots\ldots, N, \tag{15}$$

where $a_{x\max}$ and $a_{x\max}$ are the maximum and minimum value of a_{x_i}, respectively;$\Delta a_{x\max}$ and $\Delta a_{x\min}$ are the maximum and minimum value of Δa_x, respectively.

Constraints (12)-(15)guarantee the LHD stayed in the safe longitudinal corridor. Equation (13)is the velocity restriction. Equation (14) and (15) limit the longitudinal acceleration and jerk, respectively. Therefore, the smoothness and comfort can be guaranteed.

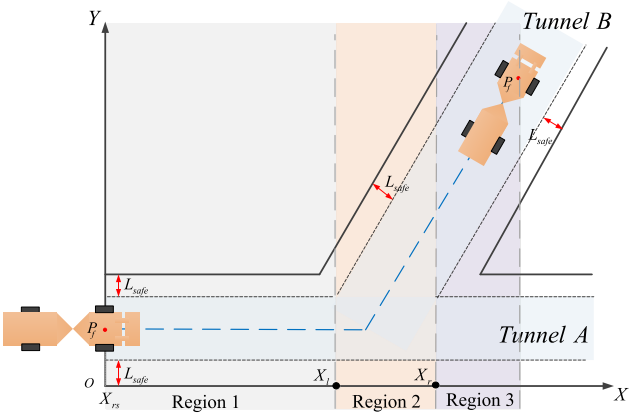

FIGURE 5. The bounds of the lateral trajectory.

B. LATERAL TRAJECTORY PLAN

1) DETERMINE THE LATERAL BOUNDS

In order to achieve safety driving, LHD must driving in the blue area. In order to define the lateral bounds, we divide the tunnel space into 3 regions, which are R_1, R_2 and R_3. Fig. 5 shows the details.

X_l and X_r are the longitudinal coordinates of the crosspoint between the safety boundaries of Tunnel B and the safe upper boundaries of Tunnel A. Region R_1 is located in tunnel A, it is the driving area before LHD enters tunnel B. R_2 is located across tunnel A and B, in which LHD will turn to tunnel B. R_3 is located in tunnel B, where the dumping point is included. R_2 and R_3 may merge into one region when tunnel A is perpendicular to tunnel B. The bounds of the longitudinal trajectory each Region are defined as follows.

The bounds of the lateral trajectory in each Region are defined as follows.

In R_1, the lateral upper and lower bounds for P_f are determined as

$$y_{\max} = D_t - L_{safe}, \quad y_{\min} = L_{safe}; \tag{16}$$

In R_2, the lateral upper and lower bounds for P_f are determined as

$$y_{\max} = a_1 x + b_1 \quad y_{\min} = L_{safe}; \tag{17}$$

In R_3, the lateral upper and lower bounds for P_f are determined as

$$y_{\max} = a_1 x + b_2, \quad y_{\min} = a_2 x + b_2, \tag{18}$$

where α is the angle between tunnel A and tunnel B. D_t is the width of tunnel A. $a_1 x + b_1$ and $a_2 x + b_2$ represent the left and right safety margin of Tunnel B, respectively.

2) OBJECTIVE FOR THE LATERAL TRAJECTORY

The objective is to minimize the lateral acceleration and the error between two successive accelerations. Therefore, the objective can be written as a quadratic function

$$J = \sum_{i=0}^{N} [\rho_1 a_{y_i}^2 + \rho_2 \Delta a_{y_i}^2], \tag{19}$$

where ρ_i, $i = 1, 2$ are the weight coefficients, $0 < \rho_i < 1 \rho_1 + \rho_2 = 1$; y_i is the lateral position of P_f; a_{y_i} is the longitudinal acceleration of P_f in x_i;$\Delta a_{y_i} = a_{y_i} - a_{y_{i-1}}$.

3) CONSTRAINTS FOR THE LATERAL TRAJECTORY

The constraints for the lateral trajectory can be divided into the following categories.

a: LATERAL MOTION CONSTRAINTS

The lateral motion can be depicted by

$$y_{i+1} = y_i + v_{y_i} \Delta t + \frac{\Delta t^2}{2} a_{y_i}, \quad i = 0, \ldots\ldots, N, \tag{20}$$

$$v_{y_{i+1}} = v_{y_i} + a_{y_i} \Delta t, \quad i = 0, \ldots\ldots, N, \tag{21}$$

where y_i is the lateral position of P_f; v_{y_i} is the lateral velocity of P_f;

In addition, LHD should satisfy the following constraints

$$y_{\min} \le y_i \le y_{\max}, \quad i = 0, \ldots\ldots, N, \tag{22}$$

$$v_{y\min} \le v_{y_i} \le v_{y\max}, \quad i = 0, \ldots\ldots, N, \tag{23}$$

$$a_{y\min} \le a_{y_i} \le a_{y\max}, \quad i = 0, \ldots\ldots, N, \tag{24}$$

$$\Delta a_{y\min} \le \Delta a_{y_i} \le \Delta a_{y\max}, \quad i = 0, \ldots\ldots, N, \tag{25}$$

where $a_{y\max}$ and $a_{y\max}$ are the maximum and minimum value of a_{y_i}, respectively; $\Delta a_{y\max}$ and $\Delta a_{y\min}$ are the maximum and minimum value of Δa_y, respectively.

Constraints (22) - (25) guarantee the LHD stayed in the safe lateral corridor. Equation (23) is the velocity restriction. Equation (24) and (25) limit the longitudinal acceleration and jerk, respectively. Therefore, the smoothness and comfort can be guaranteed.

b: ATTITUDE CONSTRAINTS AT THE END POINT

The attitude includes the heading angle of the front body and the articulated angle. The constraint of the heading angel is

$$\frac{y_N - y_{N-1}}{x_N - x_{N-1}} = \tan\theta_{fe}, \tag{26}$$

where θ_{fe} is the requirement angle of the heading angle at the end point.

For LHD, both of the two bodies' heading angles are required to keep consistent with the working direction at the end point. Therefore, the articulated angle at the end point should be as small as possible. However, since the decision variables only include the state of the front body, the articulated angle cannot be directly limited. However, since the objective function includes $\Delta a_{y_i}^2$, articulated angel will be a very small value. The case studies in Chapter 5 shows the effectiveness.

c: CONSTRAINT RELATED TO ARTICULATED ANGLE

The generated trajectory should have rationality and feasibility, which means the LHD physical constrains should be satisfied when trajectory planning. In this paper, the uniqueness lies in the constraints about the articulated angle. The articulated angle and the angular velocity have constraints. However, if the angle was chosen as the decision variable, more nonlinear constraints will be introduced inevitably, which may increase the computation burden greatly. In order to avoid this situation, the articulated angle is not used as a decision variable in this paper. In this case, in order to satisfy the articulated angle physical constraints, the heading angle has be constrained.

Based on equation(4), it can be seen that heading angular velocity $\dot{\theta}_f$ reaches the maximum when γ, $\dot{\gamma}$ and v_f reach the maximum, which is

$$\dot{\theta}_{f\max} = \frac{v_{f\max} \sin\gamma_{\max} + l_r \dot{\gamma}_{\max}}{l_f \cos\gamma_{\max} + l_r}. \tag{27}$$

With the increase of run time, $v_{f\max}$, γ and $\dot{\gamma}$ will decrease. Therefore, the value of equation (27) will decrease. Based on the above analysis, it can be known that, if $\dot{\theta}_f$ is set to a lower value than $\dot{\theta}_{f\max}$, the limitation of the articulated angel can be satisfied. In this case, the maximum value is signed as $\dot{\theta}_{f\max'}$, $\dot{\theta}_{f\max'} < \dot{\theta}_{f\max}$. In order to represent this constraints through

v_{x_i} and v_{y_i}, we have

$$\begin{aligned}
\tan\theta_{f_i} &= \frac{v_{y_i}}{v_{x_i}} \approx \tan(\theta_{f_{i-1}} + \Delta t \cdot \frac{\dot\theta_{f_i} + \dot\theta_{f_{i-1}}}{2}) \\
&\because \tan(\theta_{f_{i-1}} + \Delta t \cdot \frac{\dot\theta_{f_i} + \dot\theta_{f_{i-1}}}{2}) \\
&\quad \le \tan(\theta_{f_{i-1}} + \Delta t \cdot \frac{\dot\theta_{f_{\max}} + \dot\theta_{f_{\max}}}{2}) \\
&\because \frac{v_{y_i}}{v_{x_i}} \le \tan(\theta_{f_{i-1}} + \Delta t \cdot \frac{\dot\theta_{f_{\max}} + \dot\theta_{f_{\max}}}{2}) \\
&\quad = \frac{\tan\theta_{f_{i-1}} + \tan(\Delta t \cdot \dot\theta_{f_{\max}})}{1 - \tan\theta_{f_{i-1}} \cdot \tan(\Delta t \cdot \dot\theta_{f_{\max}})} \\
&\quad = \frac{\frac{v_{y_{i-1}}}{v_{x_{i-1}}} + \tan(\Delta t \cdot \dot\theta_{f_{\max}})}{1 - \frac{v_{y_{i-1}}}{v_{x_{i-1}}} \cdot \tan(\Delta t \cdot \dot\theta_{f_{\max}})}
\end{aligned}$$

Finally, we obtain the following constraint

$$\frac{v_{y_i}}{v_{x_i}} \le \frac{\frac{v_{y_{i-1}}}{v_{x_{i-1}}} + \tan(\Delta t \cdot \dot\theta_{f_{\max}})}{1 - \frac{v_{y_{i-1}}}{v_{x_{i-1}}} \cdot \tan(\Delta t \cdot \dot\theta_{f_{\max}})}. \tag{28}$$

d: COLLISION-FREE CONDITION

Based on the models described in section 4.1 and 4.2, the trajectory of the LHD can be obtained. However, the collision avoidance constraints of the rear body have not been discussed, which means the feasibility of the trajectory cannot be guaranteed (although a safe and reasonable trajectory of the front body can be obtained, the rear body may collide with the tunnel wall). However, if these constraints were included in the trajectory planning model, the nonlinear constraints will greatly increase the difficulty of solving the model. In order to avoid this, through in-depth analysis, the following theorem has been found and proved. Based on Theorem 1, the safety of the rear body can be guaranteed, therefore, leads to a feasible trajectory.

Theorem 1: For the LHD trajectory plan method described in section 4.1 and 4.2, when LHD turns right, if the condition (29) is satisfied; or when LHD turns left, if the condition (30) is satisfied, the trajectory obtained by the proposed method is reasonable and feasible, both of the two bodies can running safely without collision with the tunnel wall.

$$y_{flub}(x_{P_c}) \le D_{tu} - L_{safe} - D_w, \tag{29}$$

$$y_{fllb}(P_x) \ge D_{tl} + L_{safe} + D_w, \tag{30}$$

where $P_c(x_{P_c}, y_{P_c})$ is crosspoint of tunnel wall safety bounds in the direction of LHD turning; $y_{flub}(P_c)$ and $y_{fllb}(P_c)$ are the upper and lower bounds of the lateral position of front body's trajectory at point P_c, respectively; D_{tu} and D_{tl} are the lateral coordinates of left and right tunnel wall of Tunnel A, respectively; D_w is the *Difference of Radius between Inner Wheels* of the LHD.

Proof:

Because of the *Difference of Radius between Inner Wheels*, the trajectories of the two bodies are different. When LHD turns right, we have

$$y_f(x) \le y_r(x), \tag{31}$$

where $y_f(x)$ is the lateral coordinate value of the front body's trajectory when the longitudinal coordinate is x; $y_r(x)$ is the lateral coordinate value of the front body's trajectory when the longitudinal coordinate is x. When $L_f = L_r$, $y_{f(x)} = y_{r(x)}$.

During the whole journey, the most likely position for a collision is $P_c(x_{P_c}, y_{P_c})$. Therefore, at point P_c, if the upper bound of the lateral position of rear body's trajectory (signed as $y_{r(P_c)}$) is lower than y_{P_c}, the rear body will not collide with the tunnel wall. This relationship can be represent as

$$y_{r(P_x)} \le y_{P_c}. \tag{32}$$

However, the lateral coordinate of the rear body is not included in the proposed model directly. In this case, collision avoidance can be achieved by limiting the bound of the front body at P_c. It is known that the value of the *Difference of Radius between Inner Wheels* can be calculated conveniently for an LHD, and it is signed as D_w. Therefore, we have

$$y_{f(x_{P_c})} = y_{r(x_{P_c})} - D_w, \tag{33}$$

In this paper, two important items in the objective function are (1) minimizing the acceleration and (2) minimizing the difference between two successive accelerations. Therefore, the obtained trajectory must pass through P_c. The lateral upper bound of the front body's trajectory is signed as $y_{flub}(x_{P_c})$. Therefore, we have

$$y_{flub}(x_{P_c}) = y_{f(x_{P_c})}, \tag{34}$$

Substituting (33) into(34), we have

$$y_{flub}(x_{P_c}) = y_{r(x_{P_c})} - D_w, \tag{35}$$

Substituting (32) into(35), we have

$$y_{flub}(x_{P_c}) \le y_{P_c} - D_w, \tag{36}$$

Based on Fig.6, it is known that $P_y = D_{tu} - L_{safe}$, finally, we obtain

$$y_{flub}(x_{P_c}) \le D_{tu} - L_{safe} - D_w.$$

The formula we obtained is condition(29). Therefore, when (29) is satisfied, the rear trajectory according to the front body's trajectory obtained through the proposed method will not collide with the tunnel wall. Condition (30) can be obtained based on the same principle. □

Based on the objective functions and the constraints in this Chapter, we obtain the following two nonlinear optimization models.

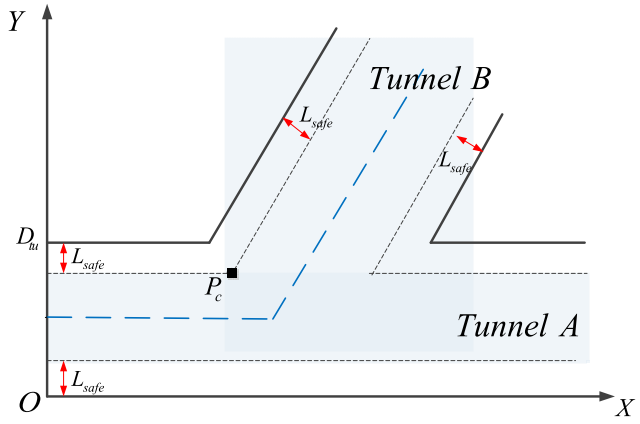

FIGURE 6. The most dangerous point (P_c) for LHD in "L" duty cycle.

For the longitudinal trajectory, we have

$$\min\ J=\sum_{i=0}^{N}[\lambda_1(v_{x_i}-v_{xdes})^2+\lambda_2 a_{x_i}^2+\lambda_3\Delta a_{x_i}^2],\quad i=0,\ldots\ldots,N,$$

$$s.t.\begin{cases} x_{i+1}=x_i+v_{x_i}\Delta t+\dfrac{\Delta t^2}{2}a_{x_i}, & i=0,\ldots\ldots,N,\\ v_{x_{i+1}}=v_{x_i}+a_{x_i}\Delta t, & i=0,\ldots\ldots,N,\\ x_{\min}\le x_i\le x_{\max}, & i=0,\ldots\ldots,N,\\ v_{x\min}\le v_{x_i}\le v_{x\max}, & i=0,\ldots\ldots,N,\\ a_{x\min}\le a_{x_i}\le a_{x\max}, & i=0,\ldots\ldots,N,\\ \Delta a_{x\min}\le\Delta a_{x_i}\le\Delta a_{x\max}, & i=0,\ldots\ldots,N. \end{cases}\tag{37}$$

For the lateral trajectory, we have

$$\min\ J=\sum_{i=0}^{N}[\rho_1 a_{y_i}^2+\rho_2\Delta a_{y_i}^2]\quad i=0,\ldots\ldots,N,$$

$$s.t.\begin{cases} y_{i+1}=y_i+v_{y_i}\Delta t+\dfrac{\Delta t^2}{2}a_{y_i}, & i=0,\ldots\ldots,N,\\ v_{y_{i+1}}=v_{y_i}+a_{y_i}\Delta t, & i=0,\ldots\ldots,N,\\ \dfrac{y_N-y_{N-1}}{x_N-x_{N-1}}=\tan\theta_{fe}. & \\ \dfrac{v_{y_i}}{v_{x_i}}\le\dfrac{\frac{v_{y_{i-1}}}{v_{x_{i-1}}}+\tan(\Delta t\cdot\dot\theta_{f\max})}{1-\frac{v_{y_{i-1}}}{v_{x_{i-1}}}\cdot\tan(\Delta t\cdot\dot\theta_{f\max})}, & i=0,\ldots\ldots,N,\\ \Delta a_{y\min}\le\Delta a_{y_i}\le\Delta a_{y\max}, & i=0,\ldots\ldots,N,\\ y_{\min}\le y_i\le y_{\max}, & i=0,\ldots\ldots,N,\\ v_{y\min}\le v_{y_i}\le v_{y\max}, & i=0,\ldots\ldots,N,\\ a_{y\min}\le a_{y_i}\le a_{y\max}, & i=0,\ldots\ldots,N. \end{cases}\tag{38}$$

From model (37) and (38), it can be seen that the coupling relationship of longitudinal and lateral trajectory is reflected in v_{x_i}. The lateral trajectory is generated based on v_{x_i}. Model (37) is a convex quadratic programming problem; therefore, any QP solver can find the solution easily. Model (38) is a nonlinear programming problem; however, there is only one type nonlinear constraint and the form is not very complex. In this paper, we apply SOP to find the solution. The general form of the two optimization problems are shown in the Appendix.

As we mentioned before, SQP is a good way to solve nonlinear optimization problem [25], [29]. SQP obtain the subproblems by Taylor expansion. In each iteration, the object is transformed into quadratic function, the equality constraints and inequality constraints are transformed into linear functions. By solving quadratic programming subproblems iteratively to obtain the solution of the origin problem.

Considering the efficiency of SQP, the size of the problem should be not too large. Usually, in order to satisfy the control requirement, the sampling interval should less than 0.2s. The economical hauling distance for LHD is less than 200m, the working velocity is around 1∼2m/s. Therefore, when $S=200$, $v=1$, the decision variables will reach the maximum. In this case, the travel time is about 200s, if $\Delta t=0.2$, then $N=T/\Delta t=200/0.2=1000$. In the planning method, the positon, velocity and acceleration of the front axle center are chosen as the decision variables, therefore, the number of decision variables are $3N$. That is to say, there will be 3000 decision variables, therefore, this optimization problem is hard to solve.

In order to overcome this, we divide the optimization process into two stages. In the first stage, the terminals states are the states of the starting and the ending point, defining N_{s1} as the number of the time intervals in the first stage and it is chosen as 50, therefore, we have

$$\Delta t_{s1}=T/50.\tag{39}$$

In the second stage, the terminals are the states of the two successive sample points of stage 1, defining N_{s2} as the number of the time intervals in the second stage.Δt_{s2} is the chosen as 0.2s, we have

$$N_{s2}=\Delta t_{s1}/0.2.\tag{40}$$

In this case, it can be known that when the running distance is 200m and the travel time is 200s,$\Delta t_{s1}=T/N_{s1}=200/50=4s$, $N_{s2}=\Delta t_{s1}/0.2=4/0.2=20$. In this situation, the maximum number of decision variables of the trajectory planning problem in the second stage is 60. That is to say, for each optimization problem in the second stage, a middle or small-scale problem can be solved effectively.

Since there are 50 time intervals in the first stage, there will be 50 longitudinal and lateral trajectory planning problems in the second stage. These may take a few seconds to solve. However, the LHD will work at the terminal (loading or dumping) for tens of second, which is long enough for the trajectory generation.

Chapter V shows the effectiveness of the proposed method through case studies.

V. CASE STUDIES AND DISSCUTION

To validate and demonstrate the effectiveness of the proposed method, we conduct a series of case studies through MATLB in a laptop with Inter Core i7CPU, 8G RAM. The longitudinal trajectory is generated through a quadratic programming model. We apply *quadprog* in Matlab to solve this problem. The lateral trajectory is generated through a nonlinear programming model. We apply *fmincon* in Matlab to solve this problem. The convergence criteria is the default.

In case 1 and 2, the starting and ending point are the same. The run time is different. In case 3, the ending point is different from case 1 and 2. Instead of choosing the midpoint of tunnel as the start point and end point, we chose two locations close to the boundary. This is also consistent with the actual situation. The working point may be in any location at the end area.

In case 4, a comparison shows the necessity of considering velocity in motion plan. The details are show as follows. The general parameters [30] of the case studies show in Table 1.

TABLE 1. The general parameters of the case studies.

Symbol	Value	SI
L_f	1.5	m
L_r	2	m
D_t	4	m
L_{safe}	0.2	m
$\dot{\theta}_{f\max}$	0.35	rad/s
$\gamma_{\max}$	0.7	rad
$\gamma_{\min}$	-0.7	rad
$\dot{\gamma}_{\max}$	0.17	rad/s
$\dot{\gamma}_{\min}$	-0.17	rad/s
α	1.05	rad
$v_{\max}$	4	m/s
$a_{x\max}$	2	m/s^2
$a_{x\min}$	-2	m/s^2
$\Delta a_{x\max}$	1.5 Δt	m/s^2
$\Delta a_{x\min}$	-3 Δt	m/s^2
$a_{y\max}$	2	m/s^2
$a_{y\min}$	-2	m/s^2
$\Delta a_{y\max}$	0.5 Δt	m/s^2
$\Delta a_{y\min}$	-0.5 Δt	m/s^2
λ_i	1/3	
ρ_i	1/2	

A. CASE 1

The experiment parameters show in Table 2.

Fig. 7 shows the spatiotemporal trajectory generated by the proposed method. The black curve is the trajectory of the front body. The green dotted curve is the longitudinal v-s trajectory. The blue dotted curve is the lateral v-s trajectory. The red dotted curve is the longitudinal-lateral location of the trajectory.

TABLE 2. Variables in case 1.

Symbol	Value	SI
X_{fs}	0	m
Y_{fs}	0	m
X_{fe}	45	m
Y_{fe}	30	m
θ_{fs}	0	rad
θ_{fe}	1.05	rad
γ_s	0	rad
T	30	s
v_{des}	2	m/s

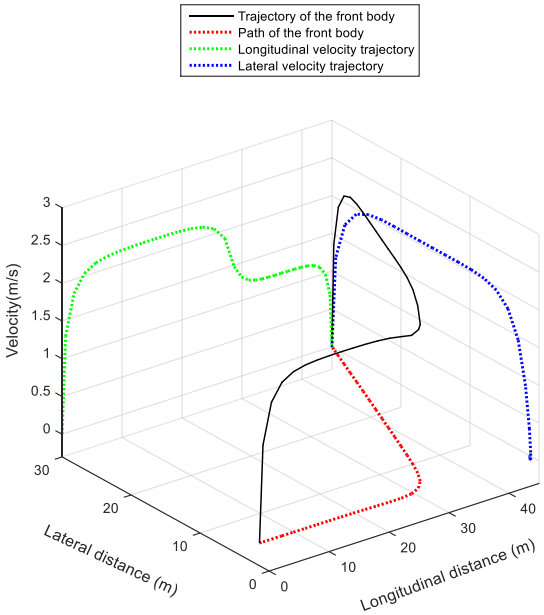

FIGURE 7. The spatiotemporal trajectory when T = 30s.

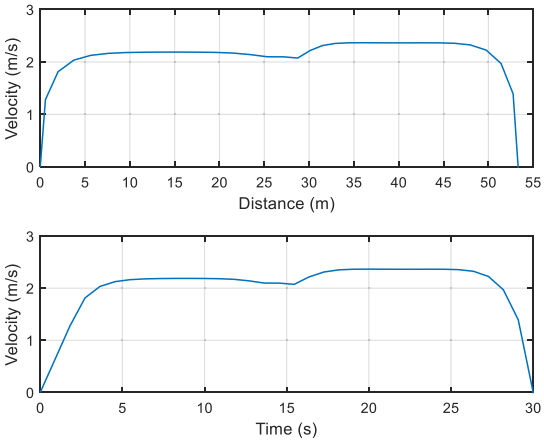

FIGURE 8. The driving velocity when T = 30s.

It is observed the longitudinal velocity decreases in the second half of the journey, the lateral velocity is very low even negative in the front half of the journey. Fig.8 is the v-s and v-t trajectory of the front body. We can observe that the velocity

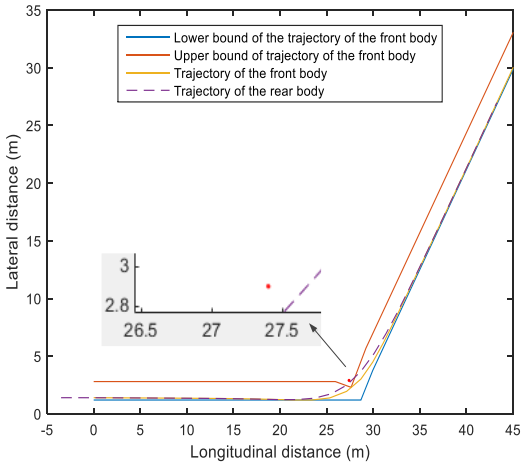

FIGURE 9. The driving velocity when T = 30s.

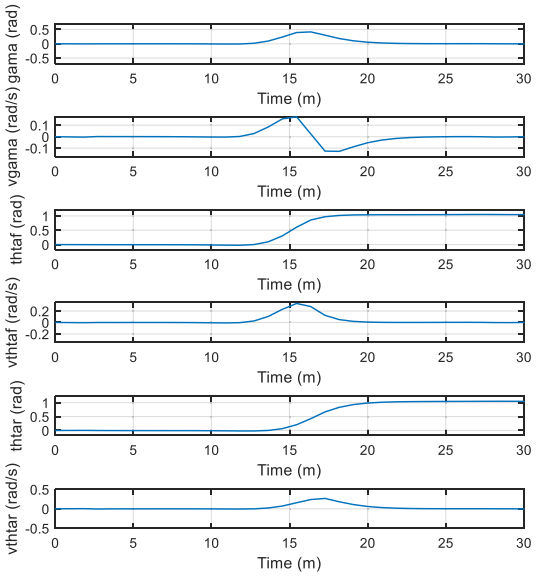

FIGURE 10. The angle and angular velocity for the three angles when T = 30s.

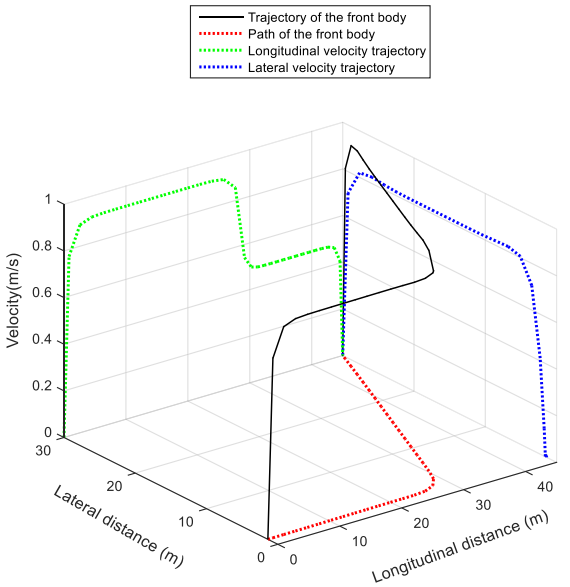

FIGURE 11. The spatiotemporal trajectory when T = 70s.

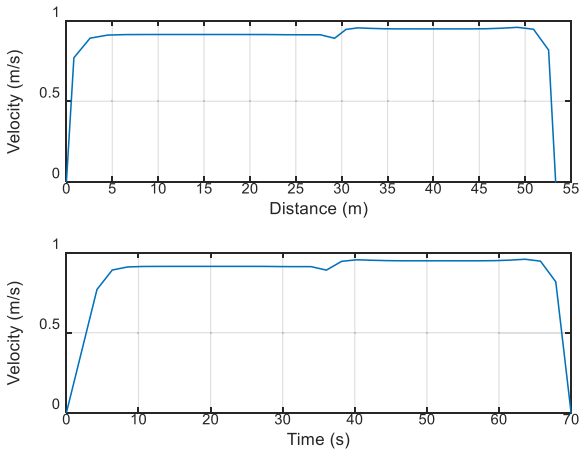

FIGURE 12. The driving velocity when T = 70s.

along the driving direction nearly remains stable, the value is about 2m/s.

From Fig.9, it is known that the negative lateral moving causes the negative lateral velocity. Since the run time is short (30s), the velocity is high. With a high velocity, the turn time is short and the required angular velocity is high. However, the articulated angular velocity has physical limitation. In this case, LHD can have a safe turn by increasing the curve radius of the driving trajectory at the junction. Therefore, it can be seen that HLD runs to the lateral lower bound at first and then turns to Tunnel B. Based on Theorem 1, the lowest value of the upper bound is set to 2.4m. We can see that the trajectory goes through this point. The red point in Fig.9 is the crossing point of the two tunnel's upper bounds. The enlarged details show that the rear body's trajectory is below this point, which means the rear body has a safe turn at the junction.

Fig.10 is the curves of the three important angles and their angular velocities. We can observe that the articulated angle and the angular velocity increases first and then decreases. In addition, both of them keep in a small value at the second half of the journey. The articulated angle at the end point is -0.01 rad, it is a very small value that can satisfy the working requirement (usually, even a human driver cannot always guarantee that the articulated angle can be 0 at the end point; Generally, the angle within ± 0.05rad can ensure the normal loading or dumping). When the angular velocity of the front body is limited to 0.35 rad/s, the range of variation for the articulated angle and its angular velocity maintains within the limitation $(-0.7rad \leq \gamma \leq 0.7rad, -0.17rad/s \leq \dot{\gamma} \leq 0.17rad/s)$, which means the obtained trajectory is reasonable and feasible. The articulated angle the angular velocity

B. CASE2

In case 2, the run time is set to 70s($T = 70$). The results are shown in Fig.11 to Fig.14. Based on Fig.11 and Fig.12, it can

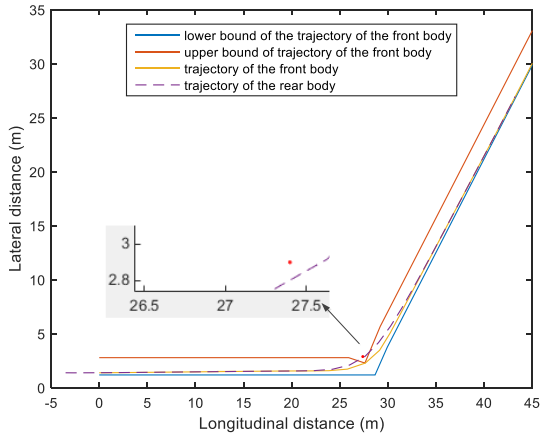

FIGURE 13. The driving velocity when T = 30s.

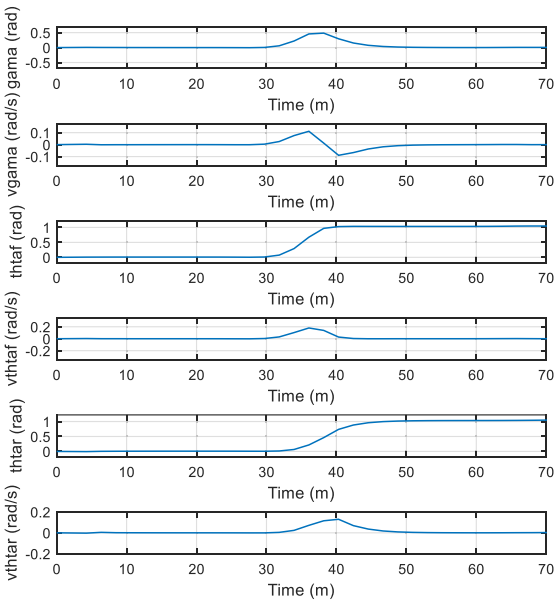

FIGURE 14. The angle and angular velocity for the three angles when T = 30s.

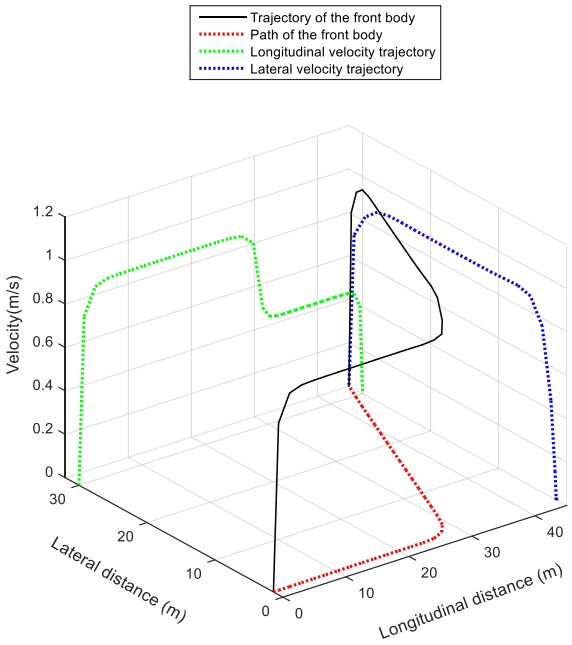

FIGURE 15. The spatiotemporal trajectory when the end is (45, 32).

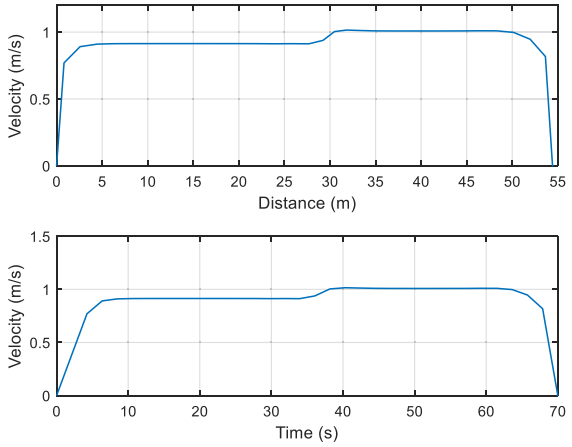

FIGURE 16. The driving velocity when the end is (45, 32).

be observed that the velocity is decreased to less than 1m/s. In Fig 11, the green dotted curve is the longitudinal v-s trajectory. The blue dotted curve is the lateral v-s trajectory. The red dotted curve is the longitudinal-lateral location of the trajectory. The trend of these curves are the same as their trend in case 1 in Case 1. There is no negative value for lateral velocity. The length of the path in this case is 53.32m.

From Fig.13, it is observed that the LHD does not drive to the lateral lower bound in Tunnel A, but directly and slowly approaches the lateral upper bound. This is because when the run time is increased, the velocity is decreased. With a lower velocity, the turn time is longer and the required angular velocity is lower. Therefore, it is unnecessary to increase the curve radius of the driving trajectory at the junction. In Fig.13, the lowest value of the upper bound is also is 2.4m. The trajectory goes through this point. The enlarged details show that the rear body's trajectory is below this point, which means the rear body has a safe turn at the junction.

Fig.14 shows the curves of the three important angles and their angular velocities. Since the run time is 70s which is two times more than 30s, the heading angular velocities of the front and rear body reduced to less than 0.17rad. We can observe that the articulated angle and the angular velocity increases first and then decreases. In addition, both of them keep in a small value at the second half of the journey. The articulated angle at the end point is -0.004 rad. The range of variation for the articulated angle and its angular velocity maintains within the limitations, which means the obtained trajectory is reasonable and feasible.

C. CASE3

In Case 3, the end point changes to (45, 32). The results are shown in Fig.15 to Fig.18. From Fig.13, we observe that the

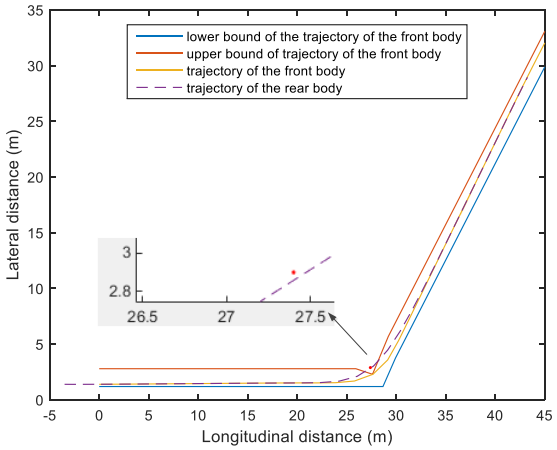

FIGURE 17. The driving velocity when the end is (45, 32).

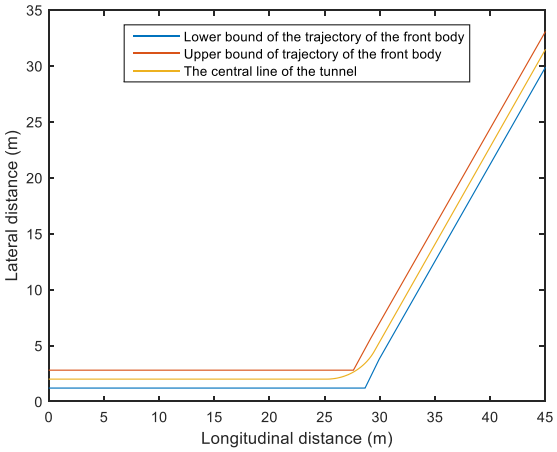

FIGURE 19. The central line of the tunnels.

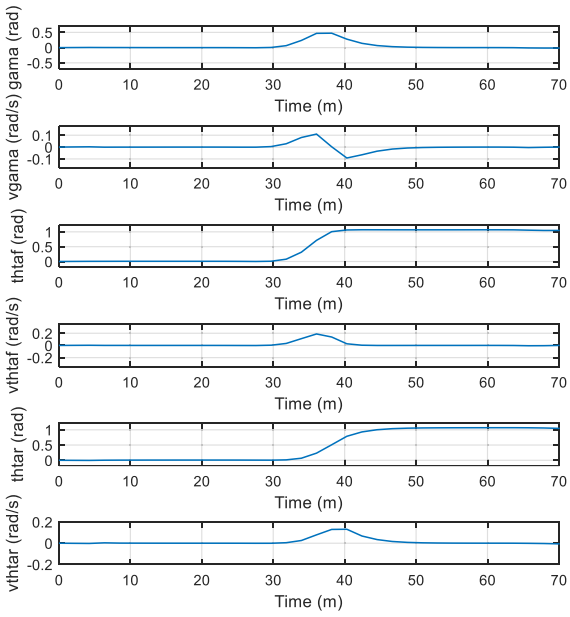

FIGURE 18. The angle and angular velocity for the three angles when the end is (45, 32).

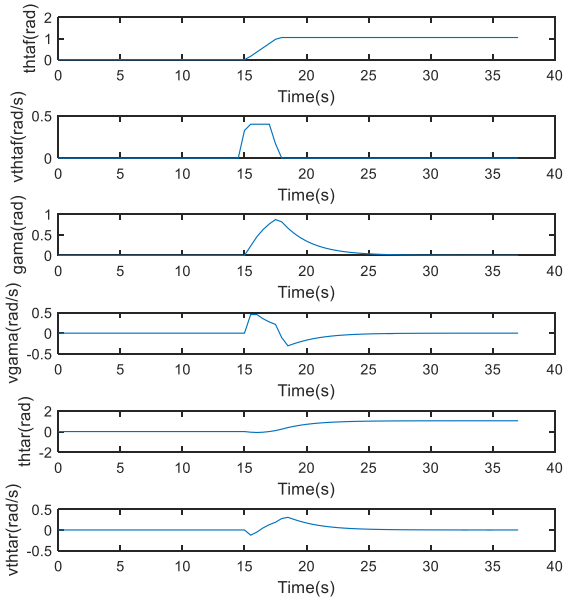

FIGURE 20. The angle and angular velocity for the three angles.

trend of the v-s curves remains the same as they are in the first two Cases. However, the velocity along the driving direction is higher the velocity in Case 2. Based on Fig.16, we notice that the driving distance is little longer than the distance in the first two Cases. In Case 3, the driving distance is 54.1m.

Since the run time remains the same (70s) and the run distance is longer, the velocity is higher.

Based on Fig.17 and Fig.18, we can see that both of the two bodies pass through the junction safely. Both of heading angles of the two bodies keep in a small value at the second half of the journey. The articulated angle at the end point is -0.03 rad. The range of variation for the articulated angle and its angular velocity still maintains within the limitations, which means the obtained trajectory is reasonable and feasible.

D. CASE4

Case 4 shows the importance and necessity of trajectory planning in practical application. Usually, the central line is the most common path for mining vehicle. However, it is not always feasible when turning. For example, we apply Line and Cycle method to connect the central lines of the two tunnels. The radius of the cycle is 5m, which is larger than the minimum steering radius of the LHD (3.57m). The path shows in Fig.19.

If the LHD tracks this path at the velocity of 2m/s without considering the articulate angular velocity limit, the curves about the three angles shows in Fig.20.

It is noticed that the articulate angular velocity exceeds maximum value (0.17rad/s). Therefore, it is impossible for the LHD to follow the central line when it is turning at the velocity of 2m/s. However, in Case 1, we can see that the

articulate angular velocity can be kept below the limit value in the junction when the driving velocity exceeds 2m/s. At the same time, we observes that the path of the LHD is not the central line. Therefore, it is very important to consider velocity for seeking a feasible trajectory.

Furthermore, even if the physical constraint of the articulated angular velocity is fast enough, the central line is still not a feasible path. Unless the length of the front body and rear body are the same, otherwise, the rear body will collide with the tunnel wall due to the Difference of Radius between Inner Wheels.

In addition, in order to pass the junction, we can set section speeds, low speed for turning, and high speed for straight driving. However, where to start slowing down, and what the velocity it should be are need to be decided through some scientific methods. Otherwise, the production efficiency and energy consumption will be affected.

Based on these case studies, it is known that velocity is also an important factor in motion plan. Only planning a path cannot satisfy the requirements of efficient and safe production. For autonomous LHD, a planning method is needed to find the spatiotemporal trajectory, which is the contribution of this paper. Since the longitudinal trajectory plan model is convex and the nonlinear constraints of the lateral trajectory plan model are not very complex, the computation time is short. The trajectory can be obtained within a few seconds. The computational time of Case 1to Case 3 are listed in Table 3.

TABLE 3. The computational time of the cases.

	Case 1		*Case 2*		*Case 3*	
	Longitudinal	Lateral	Longitudinal	Lateral	Longitudinal	Lateral
N_{s1}	50	50	50	50	50	50
Δt_{s1}	0.6s	0.6s	1.4s	1.4s	1.4s	1.4s
Number of the decision variables	150	150	150	150	150	150
Computational time	0.01	2.67	0.02	3.46	0.02	3.62
N_{s2}	3	3	7	7	7	7
Δt_{s2}	0.2s	0.2s	0.2s	0.2s	0.2s	0.2s
Number of the decision variables	9	9	21	21	21	21
Average computational time	Less than 0.01s	0.06	Less than 0.01s	0.21	Less than 0.01s	0.21

The longitudinal trajectory planning problem is convex, convergence is widely known. The lateral trajectory problem is a nonlinear programming problem with quadratic objective, linear equality constraints and nonlinear inequality constraints. In addition, in the first optimization stage, there

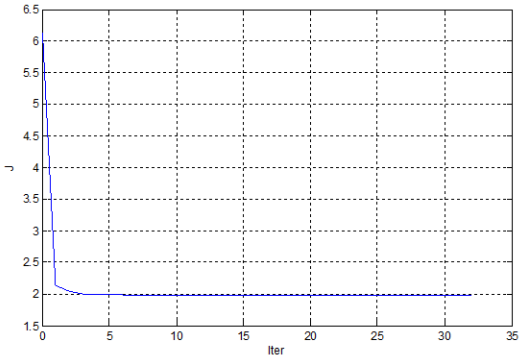

FIGURE 21. The first stage lateral trajectory convergence plot of Case1.

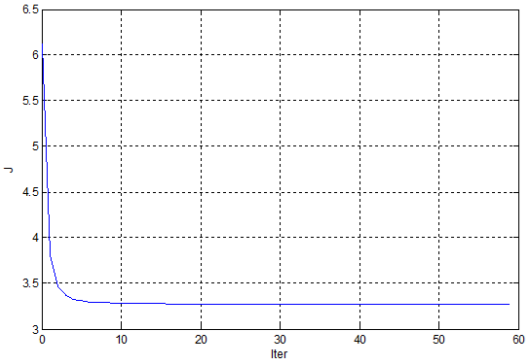

FIGURE 22. The first stage lateral trajectory convergence plot of Case2.

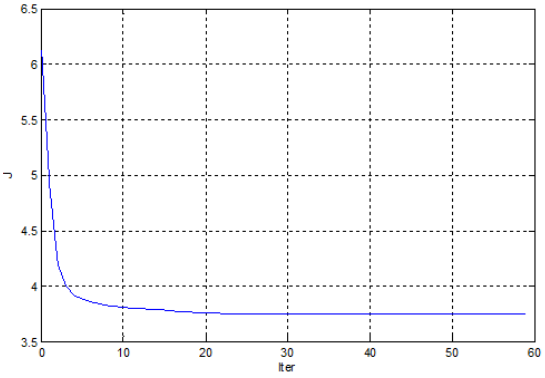

FIGURE 23. The first stage lateral trajectory convergence plot of Case3.

are 150 decision variables. These are the most complicated problem in this article. Therefore, we show the convergence plots of the lateral trajectory optimization in the first stage for Case 1 to Case 3 in Fig.21 to Fig.23.

It can be seen that, for Case 1, the solution can be obtained after 10 iterations; for Case 2 and 3, the solution can be obtained after 20 iterations. Therefore, the computational time for Case 1 is shorter. Although the number of the decision variables are the same, the computational time are different. This may cause by the different driving time. In Case 1, the driving time is 30s; in Case 2 and 3,

the driving time is 70s. The longer the driving time, the larger the search space, therefore, leading to a longer computational time.

At the end of this Chapter, we analyze a phenomenon of a trajectory generated by this method. Form these cases, it is noticed that there is a fluctuation in velocity at the junction. The setting of the desired velocity mainly causes this. In this paper, the desired velocity is set by $v_{des} = S/T$. S is the length of the trajectory. Since we didn't know the exact length of the trajectory before trajectory planning, S is set to a constant value (60m) for these cases. Therefore, v_{des} is a constant value. In Tunnel A, $v_{xdes} = v_{des}$; in Tunnel B, $v_{xdes} = v_{des} \cdot \cos\alpha$. In this way, the longitudinal desired velocity suddenly goes down at the junction, at the same time, the lateral bound goes up suddenly. Therefore, the velocity may fluctuate at the junction. In order to improve this problem, how to set the desired velocity is an improvement direction for this method.

VI. CONCLUSION AND FORECAST

In this paper, the local trajectory plan problem for LHD's most common working scenario has been deeply investigated. A novel trajectory planning method based on longitudinal and lateral trajectory planning is proposed. This method has two special characteristics: (1) no angles are included in the decision variables; (2) collision avoidance constraints of the rear body is not directly considered in the planning model, but ensured through a rationality and feasibility condition. For the LHD's duty cycle, the length of economic haul is less than 200m, the driving velocity is about 1m/s∼2m/s. Through the method, the number and complexity of the nonlinear constraints can keep in a reasonable level. All these advantages make the proposed method easy to implement. Case studies show the effectiveness of the proposed method. With the proposed method, the intelligent degree of LHD will be promoted, which is conducive to the development of intelligent mining.

According to the characteristics of LHD trajectory planning problem, with a single method, nonlinear programming is the most suitable method. Under this frame, the more targeted solving algorithm is worth studying. Compare with the SQP, CFS is more efficient on trajectory generation. Inspired by this idea, how to make feasible domain convex in the case of time varying LHD size is the research focus. In addition, based on the exiting trajectory planning method, the compound trajectory method combining more than two exiting methods maybe a feasible way. The whole process can be divided into several subsegments. In this case, how to consider various constraints and terminal requirements are the problems need to be solved.

APPENDIX

(1) The longitudinal trajectory planning problem is a convex quadratic programming problem. The vector of decision parameters is $\mathbf{x}$, $\mathbf{x} = [x_1, \cdots, x_N, v_{x1}, \cdots, v_{xN}, a_{x1}, \cdots, a_{xN}]$. The general form can be expressed as

$$\min\ J(\mathbf{x}) = \frac{1}{2}\mathbf{x}^{\mathrm{T}}\mathbf{H}_{\mathrm{x}}\mathbf{x} + \mathbf{f}_{\mathrm{x}}^{\mathrm{T}}\mathbf{x} + N\lambda_1 v_{xdes}^2 \quad \begin{cases} \mathbf{A_{eq}x} = \mathbf{B_{eq}}, \\ \mathbf{A}\mathrm{x} \le \mathbf{B}, \\ \mathbf{lb} \le \mathbf{x} \le \mathbf{ub}. \end{cases} \tag{A1}$$

$\mathbf{H}$ is a 3N × 3N matrix and

$$\mathbf{H}_{\mathrm{x}} = \begin{pmatrix} \mathbf{H}_{x1} & & \\ & \mathbf{H}_{x2} & \\ & & \mathbf{H}_{x3} \end{pmatrix}.$$

$\mathbf{H_{x1}}$, $\mathbf{H_{x1}}$ and $\mathbf{H_{x1}}$ are the matrix of N × N.

$$\mathbf{H_{x1}} = \begin{pmatrix} 0 & \cdots & 0 \\ \vdots & \ddots & \vdots \\ 0 & \cdots & 0 \end{pmatrix}, \quad \mathbf{H}_{x2} = \begin{pmatrix} \lambda_1 & \cdots & 0 \\ \vdots & \ddots & \vdots \\ 0 & \cdots & \lambda_1 \end{pmatrix},$$

$$\mathbf{H}_{x3} = \begin{pmatrix} 2(\lambda_2+\lambda_3) & -2\lambda_3 & & & \\ -2\lambda_3 & 2(\lambda_2+2\lambda_3) & \ddots & & \\ & -2\lambda_3 & \ddots & -2\lambda_3 & \\ & & \ddots & 2(\lambda_2+2\lambda_3) & \\ & & & -2\lambda_3 & 2\lambda_3 \end{pmatrix}.$$

$\mathbf{f}_{\mathrm{x}}$ is a 1 × 3N row vector, $\mathbf{f}_{\mathrm{x}} = [\,\mathbf{f}_{\mathrm{x1}}\ \mathbf{f}_{\mathrm{x2}}\ \mathbf{f}_{\mathrm{x1}}\,]$. $\mathbf{f}_{\mathrm{x1}}$ and $\mathbf{f}_{\mathrm{x2}}$ are two 1 × N row vectors.

$\mathbf{f}_{\mathrm{x1}} = [0, \cdots, 0]$, $\mathbf{f}_{\mathrm{x2}} = [-2\lambda_1 v_{xdes}, \cdots, -2\lambda_1 v_{xdes}]$.

The linear equality constraints are $\mathbf{A_{eq}x} = \mathbf{B_{eq}}$, where

$$\mathbf{A_{eq}} = \begin{pmatrix} \mathbf{A_{eq1}} & \mathbf{A_{eq2}} & \mathbf{A_{eq3}} \\ \mathbf{A_{eq4}} & \mathbf{A_{eq5}} & \mathbf{A_{eq6}} \end{pmatrix} \tag{A2}$$

where $\mathbf{A_{eq1}}$ to $\mathbf{A_{eq6}}$ are six N × N matrix.

$$\mathbf{A_{eq1}} = \begin{pmatrix} 1 & -1 & & \\ & \ddots & & \\ & & 1 & -1 \\ & & & 1 \end{pmatrix},$$

$$\mathbf{A_{eq2}} = \begin{pmatrix} \Delta t & & & \\ & \ddots & & \\ & & \Delta t & \\ & & & 0 \end{pmatrix}, \quad \mathbf{A_{eq3}} = \begin{pmatrix} \Delta t^2/2 & & & \\ & \ddots & & \\ & & \Delta t^2/2 & \\ & & & 0 \end{pmatrix},$$

$$\mathbf{A_{eq4}} = \begin{pmatrix} 1 & -1 & & \\ & \ddots & \ddots & \\ & & \ddots & -1 \\ & & & 1 \end{pmatrix}, \quad \mathbf{A_{eq5}} = \begin{pmatrix} \Delta t & & & \\ & \ddots & & \\ & & \Delta t & \\ & & & 0 \end{pmatrix},$$

$$\mathbf{A_{eq6}} = \begin{pmatrix} 0 & & \\ & \ddots & \\ & & 0 \end{pmatrix}.$$

$$\mathbf{B_{eq}^{T}} = [\,\mathbf{B_{eq1}} \quad \mathbf{B_{eq2}}\,], \tag{A3}$$

where $\mathbf{B_{eq1}}$ and $\mathbf{B_{eq2}}$ are two 1 × N row vectors.

$$\mathbf{B_{eq1}} = [0, \cdots, 0, X_{fe}]$$
$$\mathbf{B_{eq2}} = [0, \cdots, 0]$$

The linear inequality constraints are $\mathbf{Ax} = \mathbf{B}$, where

$$\mathbf{A} = \begin{pmatrix} \mathbf{A}_1 & \mathbf{A}_1 & \mathbf{A}_2 \\ \mathbf{A}_1 & \mathbf{A}_1 & \mathbf{A}_3 \end{pmatrix}, \tag{A4}$$

where $\mathbf{A}_1$ to $\mathbf{A}_3$ are three N × N matrix.

$$\mathbf{A}_1 = \begin{pmatrix} 0 & & \\ & \ddots & \\ & & 0 \end{pmatrix}, \quad \mathbf{A}_2 = \begin{pmatrix} -1 & 1 & & \\ & \ddots & \ddots & \\ & & -1 & 1 \\ & & & 0 \end{pmatrix},$$
$$\mathbf{A}_3 = \begin{pmatrix} 1 & -1 & & \\ & \ddots & \ddots & \\ & & 1 & -1 \\ & & & 0 \end{pmatrix}.$$
$$\mathbf{B^T} = \begin{bmatrix} \mathbf{B_1} & \mathbf{B_2} \end{bmatrix},$$

where $\mathbf{B}_1$ and $\mathbf{B_2}$ are two 1 × N row vectors.

$$\mathbf{B}_1 = \begin{bmatrix} \Delta a_{\max} & \cdots & \Delta a_{\max} \end{bmatrix},$$
$$\mathbf{B}_2 = \begin{bmatrix} \Delta a_{\min} & \cdots & \Delta a_{\min} \end{bmatrix}.$$

The lower bounds of $\mathbf{x}$ is $\mathbf{lb}$, $\mathbf{lb^T}$=[$\mathbf{lb}_1$ $\mathbf{lb}_2$ $\mathbf{lb}_3$], where $\mathbf{lb}_1$ to $\mathbf{lb}_3$ are two 1 × N row vectors.

$$\mathbf{lb}_1 = [x_{\min}, \cdots, x_{\min}],$$
$$\mathbf{lb}_2 = [v_{x\,\min}, \cdots, v_{x\,\min}],$$
$$\mathbf{lb}_3 = [a_{x\,\min}, \cdots, a_{x\,\min}].$$

The upper bounds of $\mathbf{x}$ is $\mathbf{ub}$, $\mathbf{ub^T}$=[$\mathbf{ub_1}$ $\mathbf{ub_2}$ $\mathbf{ub_3}$], where $\mathbf{ub}_1$ to $\mathbf{ub}_3$ are two 1 × N row vectors.

$$\mathbf{ub}_1 = [x_{\min}, \cdots, x_{\min}],$$
$$\mathbf{ub}_2 = [v_{x\,\min}, \cdots, v_{x\,\min}],$$
$$\mathbf{ub}_3 = [a_{x\,\min}, \cdots, a_{x\,\min}].$$

(2) The lateral trajectory planning problem is a nonlinear programming problem. The vector of decision parameters is $\mathbf{y}$, $\mathbf{y} = [y_1, \cdots, y_N, v_{y1}, \cdots, v_{yN}, a_{y1}, \cdots, a_{yN}]$. The general form can be expressed as

$$\min\ J(\mathbf{y}) = \frac{1}{2}\mathbf{y}^{\mathrm{T}}\mathbf{H}_{\mathrm{y}}\mathbf{y}$$
$$\begin{cases} \mathbf{A_{eq}y} = \mathbf{B_{eq}}, \\ \mathbf{Ay} \le \mathbf{B}, \\ \frac{1}{2}\mathbf{y}^{\mathrm{T}}\mathbf{H}_{\mathrm{y'}}\mathbf{y} + \mathbf{f}_{\mathrm{y'}}^{\mathrm{T}}\mathbf{y} \le \mathbf{C}, \\ \mathbf{lb} \le \mathbf{y} \le \mathbf{ub}. \end{cases}$$

$\mathbf{H}$ is a 3N × 3N matrix and

$$\mathbf{H}_{\mathrm{y}} = \begin{pmatrix} \mathbf{H}_{\mathrm{y1}} & & \\ & \mathbf{H}_{\mathrm{y1}} & \\ & & \mathbf{H}_{\mathrm{y2}} \end{pmatrix}.$$

$\mathbf{H_{y1}}$ and $\mathbf{H}_{\mathrm{y2}}$ is the matrix of N × N.

$$\mathbf{H_{y1}} = \begin{pmatrix} 0 & \cdots & 0 \\ \vdots & \ddots & \vdots \\ 0 & \cdots & 0 \end{pmatrix},$$
$$\mathbf{H}_{\mathrm{y2}} = \begin{pmatrix} 2(\rho_1+\rho_2) & -2\rho_2 & & & \\ -2\rho_2 & 2(\rho_1+2\rho_2) & \ddots & & \\ & -2\rho_2 & \ddots & -2\rho_2 & \\ & & \ddots & 2(\rho_1+2\rho_2) & \\ & & & -2\rho_2 & 2\rho_2 \end{pmatrix}.$$

The linear equality constraints are $\mathbf{A_{eq}y} = \mathbf{B_{eq}}$, where

$$\mathbf{A_{eq}} = \begin{pmatrix} \mathbf{A_{eq1}} & \mathbf{A_{eq2}} & \mathbf{A_{eq3}} \\ \mathbf{A_{eq4}} & \mathbf{A_{eq5}} & \mathbf{A_{eq6}} \\ \mathbf{A_{eq7}} & \mathbf{A_{eq6}} & \mathbf{A_{eq6}} \end{pmatrix},$$

where $\mathbf{A_{eq1}}$ to $\mathbf{A_{eq6}}$ are the same as expression (A2). $\mathbf{A_{eq7}}$ is a 1 × N row vector, $\mathbf{A_{eq7}} = [\,0 \cdots -1\ 1\,]$.

$\mathbf{B_{eq}^T}$=[$\mathbf{B_{eq1}}$ $\mathbf{B_{eq2}}$ $\mathbf{B_{eq3}}$], where $\mathbf{B_{eq1}}$ to $\mathbf{B_{eq3}}$ are three 1 × N row vectors.$\mathbf{B_{eq1}}$ and $\mathbf{B_{eq2}}$ are the same as expression (A3), $\mathbf{B_{eq3}}$ is a 1 × N row vector, $\mathbf{B_{eq3}} = [(x_N - x_{N-1})\tan\theta_{fe}, 0, \cdots, 0]$.

The linear inequality constraints is $\mathbf{Ay} = \mathbf{B}$, where $\mathbf{A}$ and $\mathbf{B}$ are the same as expression (A4) and (A5).

$$\mathbf{H}_{\mathrm{y'}} = \begin{pmatrix} \mathbf{H}_{\mathrm{y'_1}} & \mathbf{H}_{\mathrm{y'_1}} & \mathbf{H}_{\mathrm{y'_1}} \\ \mathbf{H}_{\mathrm{y'_1}} & \mathbf{H}_{\mathrm{y'_2}} & \mathbf{H}_{\mathrm{y'_1}} \\ \mathbf{H}_{\mathrm{y'_1}} & \mathbf{H}_{\mathrm{y'_1}} & \mathbf{H}_{\mathrm{y'_1}} \end{pmatrix}, \quad \mathbf{H}_{\mathrm{y'_1}} = \begin{pmatrix} 0 & & \\ & \ddots & \\ & & 0 \end{pmatrix},$$
$$\mathbf{H}_{\mathrm{y'2}} = \begin{pmatrix} 0 & -\tan(\Delta t \cdot \dot{\theta}_{f\max}) & & \\ -2\tan(\Delta t \cdot \dot{\theta}_{f\max}) & \ddots & \ddots & \\ & & \ddots & -\tan(\Delta t \cdot \dot{\theta}_{f\max}) \\ & & -2\tan(\Delta t \cdot \dot{\theta}_{f\max}) & 0 \end{pmatrix}$$
$$\mathbf{f}_{\mathrm{y'}} = [\,\mathbf{f}_{\mathrm{y'1}} \quad \mathbf{f}_{\mathrm{y'2}} \quad \mathbf{f}_{\mathrm{y'1}}\,], \mathbf{f}_{y'1} = [\,0 \quad \cdots \quad 0\,],$$
$$\mathbf{f}_{y'2} = [-2\,v_{x2} \quad -2(v_{x1} - v_{x3}) \quad \cdots \quad -2(v_{xN} - v_{x(N-2)}) \quad 2v_{x(N-1)}\,]$$

The linear inequality constraints are $\frac{1}{2}\mathbf{y}^{\mathrm{T}}\mathbf{H}_{y'}\mathbf{y} + \mathbf{f}_{y}^{\mathrm{T}}\mathbf{y} \leq \mathbf{C}$. $\mathbf{H}_{y'}$ is a 3N × 3N matrix, $\mathbf{H}_{y'}$, $\mathbf{H}_{y'_1}$, $\mathbf{H}_{y'2}$, $\mathbf{f}_{y'}$, and $\mathbf{f}_{y'2}$ are shown at the bottom of the previous page.

$\mathbf{C}$ is a $1 \times N$ row vector

$$\mathbf{C}^{\mathrm{T}} = [0, v_{x1}v_{x2}\tan(\Delta t \cdot \dot{\theta}_{f_{\max}}), \cdots, v_{x(N-1)}v_{xN} \times \tan(\Delta t \cdot \dot{\theta}_{f_{\max}}), 0].$$

REFERENCES

[1] J. M. Roberts, E. S. Duff, and P. I. Corke, "Reactive navigation and opportunistic localization for autonomous underground mining vehicles," *Inf. Sci.*, vol. 145, nos. 1–2, pp. 127–146, Aug. 2002. doi: 10.1016/s0020-0255(02)00227-x.

[2] D. González, J. Pérez, V. Milanés, and F. Nashashibi, "A review of motion planning techniques for automated vehicles," *IEEE Trans. Intell. Transp. Syst.*, vol. 17, no. 4, pp. 1135–1145, Apr. 2016. doi: 10.1109/tits.2015.2498841.

[3] S. Dixit, S. Fallah, U. Montanaro, M. Dianati, A. Stevens, F. Mccullough, and A. Mouzakitis, "Trajectory planning and tracking for autonomous overtaking: State-of-the-art and future prospects," *Annu. Rev. Control*, vol. 45, pp. 76–86, Mar. 2018. doi: 10.1016/j.arcontrol.2018.02.001.

[4] U. Andersson, K. Mrozek, K. Hyyppä, and K. Åström, "Path design and control algorithms for articulated mobile robots," in *Proc. FSR*, London, U.K., 1998, pp. 390–396. doi: 10.1007/978-1-4471-1273-0_59.

[5] F. Ma, H. Yang, Q. Gu, and Y. Meng, "Navigation path planning of unmanned underground LHD based on improved a algorithm," *Trans. Chin. Soc. for Agricult. Machinery*, vol. 46, no. 07, pp. 303–309, 2015. doi: 10.6041/j.issn.1000-1298.2015.07.043.

[6] J.-W. Choi and K. Huhtala, "Constrained global path optimization for articulated steering vehicles," *IEEE Trans. Veh. Technol.*, vol. 65, no. 4, pp. 1868–1879, Apr. 2016. doi: 10.1109/TVT.2015.2424933.

[7] H. Ishimoto, T. Tsubouchi, S. Sarata, and S. I. Yuta, "A practical trajectory following of an articulated steering type vehicle," in *Proc. FSR*, London, U.K., 1998, pp. 397–404. doi: 10.1007/978-1-4471-1273-0_60.

[8] W. Yossawee, T. Tsubouchi, S. Sarata, and S. Yuta, "Path generation for articulated steering type vehicle using symmetrical clothoid," in *Proc. IEEE-ICIT*, Bangkok, Thailand, Dec. 2002, pp. 187–192.

[9] T. Nayl, G. Nikolakopoulos, and T. Gustafsson, "Effect of kinematic parameters on MPC based on-line motion planning for an articulated vehicle," *Robot. Auton. Syst.*, vol. 70, pp. 16–24, Aug. 2015. doi: 10.1016/j.robot.2015.04.005.

[10] T. Nayl, G. Nikolakopoulos, and T. Gustafsson, "On-line path planning for an articulated vehicle based on model predictive control," in *Proc. IEEE CCA.*, New York, NY, USA, Aug. 2013, pp. 772–777. doi: 10.1109/CCA.2013.6662843.

[11] R. Hult and R. S. Tabar, "Path planning for highly automated vehicles," M.S. thesis, Dept. Signals Syst., Chalmers Univ. Technol., Göteborg, Sweden, 2013.

[12] S. Glaser, B. Vanholme, S. Mammar, D. Gruyer, and L. Nouveliere, "Maneuver-based trajectory planning for highly autonomous vehicles on real road with traffic and driver interaction," *IEEE Trans. Intell. Transp. Syst.*, vol. 11, no. 3, pp. 589–606, Sep. 2010.

[13] S. Kitazawa and T. Kaneko, "Control target algorithm for direction control of autonomous vehicles in consideration of mutual accordance in mixed traffic conditions," in *Proc. 13th AVEC*, Munich, Germany, 2016, p. 151.

[14] D. Dolgov, S. Thrun, M. Montemerlo, and J. Diebel, "Practical search techniques in path planning for autonomous driving," in *Proc. 1st Int. Symp. Search Techn. Arterial Intell. Robot. (STAIR)*, Ann Arbor, MI, USA, Jun. 2008, pp. 18–80.

[15] L. E. Kavraki, P. Svestka, J.-C. Latombe, and M. H. Overmars, "Probabilistic roadmaps for path planning in high-dimensional configuration spaces," *IEEE Trans. Robot. Automat.*, vol. 12, no. 4, pp. 566–580, Aug. 1996. doi: 10.1109/70.508439.

[16] S. M. LaValle and J. J. Kuffner, Jr., "Randomized kinodynamic planning," *Int. J. Robot. Res.*, vol. 20, no. 5, pp. 378–400, May 2001.

[17] S. Karaman and E. Frazzoli, "Optimal kinodynamic motion planning using incremental sampling-based methods," in *Proc. 49th IEEE CDC*, Atlanta, GA, USA, Dec. 2010, pp. 7681–7687. doi: 10.1109/CDC.2010.5717430.

[18] D. Dolgov, S. Thrun, M. Montemerlo, and J. Diebel, "Path planning for autonomous vehicles in unknown semi-structured environments," *Int. J. Robot. Res.*, vol. 29, no. 5, pp. 485–501, Apr. 2010. doi: 10.1177/0278364909359210.

[19] J. Ziegler, M. Werling, and J. Schroder, "Navigating car-like robots in unstructured environments using an obstacle sensitive cost function," in *Proc. IEEE Intell. Vehicles Symp.*, Eindhoven, The Netherlands, Jun. 2008, pp. 787–791. doi: 10.1109/IVS.2008.4621302.

[20] J. Ziegler and C. Stiller, "Spatiotemporal state lattices for fast trajectory planning in dynamic on-road driving scenarios," in *Proc. IEEE/RSJ Int. Conf. IROS*, St. Louis, MO, USA, Oct. 2009, pp. 1879–1884. doi: 10.1109/IROS.2009.5354448.

[21] T. Gu, J. Snider, J. M. Dolan, and J.-W. Lee, "Focused trajectory planning for autonomous on-road driving," in *Proc. IEEE Intell. Vehicles Symp. (IV)*, Gold Coast, QLD, Australia, Jun. 2013, pp. 547–552. doi: 10.1109/IVS.2013.6629524.

[22] M. Werling, S. Kammel, J. Ziegler, and L. Gröll, "Optimal trajectories for time-critical street scenarios using discretized terminal manifolds," *Int. J. Robot. Res.*, vol. 31, no. 3, pp. 346–359, Mar. 2012. doi: 10.1177/0278364911423042.

[23] M. Werling, J. Ziegler, S. Kammel, and S. Thrun, "Optimal trajectory generation for dynamic street scenarios in a Frenét Frame," in *Proc. IEEE ICRA*, Anchorage, AK, USA, May 2010, pp. 987–993. doi: 10.1109/ROBOT.2010.5509799.

[24] A. Carvalho, Y. Q. Gao, A. Gray, H. E. Tseng, and F. Borrelli, "Predictive control of an autonomous ground vehicle using an iterative linearization approach," in *Proc. 16th Int. IEEE Conf. ITSC.*, The Hague, Netherlands, Oct. 2013, pp. 2335–2340.

[25] J. Ziegler *et al.*, "Making bertha drive—An autonomous journey on a historic route," *IEEE Intell. Transp. Syst. Mag.*, vol. 6, no. 2, pp. 8–20, Apr. 2014. doi: 10.1109/mits.2014.2306552.

[26] J. Ziegler, P. Bender, T. Dang, and C. Stiller, "Trajectory planning for Bertha—A local, continuous method," in *Proc. IEEE IV Symp.*, Dearborn, MI, USA, Jun. 2014, pp. 450–457. doi: 10.1109/IVS.2014.6856581.

[27] C. Liu, C. Lin, and M. Tomizuka, "The convex feasible set algorithm for real time optimization in motion planning," *SIAM J. Control Optim.*, vol. 56, no. 4, pp. 2712–2733, Jun. 2018. doi: 10.1137/16M1091460.

[28] C. Liu, C.-Y. Lin, Y. Wang, and M. Tomizuka, "Convex feasible set algorithm for constrained trajectory smoothing," in *Proc. Amer. Control Conf. (ACC)*, Seattle, WA, USA, May 2017, pp. 4177–4182. doi: 10.23919/ACC.2017.7963597.

[29] W. Lim, S. Lee, M. Sunwoo, and K. Jo, "Hierarchical trajectory planning of an autonomous car based on the integration of a sampling and an optimization method," *IEEE Trans. Intell. Transp. Syst.*, vol. 19, no. 2, pp. 613–626, Feb. 2018. doi: 10.1109/TITS.2017.2756099.

[30] J. Nilsson, M. Brännström, J. Fredriksson, and E. Coelingh, "Longitudinal and lateral control for automated yielding maneuvers," *IEEE Trans. Intell. Transp. Syst.*, vol. 17, no. 5, pp. 1404–1414, May 2016. doi: 10.1109/TITS.2015.2504718.

[31] G. Bai, L. Liu, Y. Y. Meng, and W. Q. B. Luo Gu Ma, "Path tracking of mining vehicles based on nonlinear model predictive control," *Appl. Sci.*, vol. 9, no. 7, p. 1372, Apr. 2019.

QING GU received the Ph.D. degree in intelligent traffic engineering from Beijing Jiaotong University, Beijing, China, in 2014. She has been a Visiting Scholar with California PATH, University of California, Berkeley, CA, USA. She is currently an Assistant Professor with the School of Mechanical Engineering, University of Science and Technology Beijing, Beijing. Her research interests include systems modeling, and control and optimization with application in intelligent transportation system.

LI LIU received the Ph.D. degree in mechanical engineering from the University of Science and Technology Beijing, Beijing, China, in 2012, where he is currently a Professor with the School of Mechanical Engineering. His research interests include autonomous driving and mine intelligence.

GUOXING BAI received the B.Eng. degree in vehicle engineering from Northeastern University, Shenyang, China, in 2014. He is currently pursuing the Ph.D. degree in mechanical engineering with the University of Science and Technology Beijing, Beijing, China. His research interests include the path tracking control and model predictive control.

KAILUN LI received the B.Eng. degree in mechatronic engineering from the Shandong University of Technology, Zibo, China, in 2018. He is currently pursuing the MA.Eng. degree in mechanical engineering with the University of Science and Technology Beijing, Beijing, China. His research interest includes path planning and tracking.

YU MENG received the M.S. and Ph.D. degrees in computer science and technology from Jilin University, Changchun, China, in 2007. He is currently an Associate Professor with the School of Mechanical Engineering, University of Science and Technology Beijing, Beijing, China. His research interests include computer vision and intelligent vehicle.

FEI MA received the Ph.D. degree in automotive engineering from the University of Science and Technology Beijing, Beijing, China, in 2005, where he is currently a Professor and the Director of the School of Mechanical Engineering.

He has participated in several major projects on intelligent vehicles funded by the Chinese Government. His research interests include intelligent mining systems, vehicle vibration noise analysis and control, fault detection and diagnosis, system reliability and safety, and system-level fail-safe.